Hybrid RANS/PDF calculations of Sydney Swirling Flames

R. De Meester[1]*, B. Naud[2], B. Merci[1]

[1]Ghent University - UGent, Department of Flow, Heat and Combustion Mechanics, Ghent, Belgium
[2] Modeling and Numerical Simulation Group, Energy Dept., Ciemat, Madrid, Spain

Abstract

In this work, we perform steady 2D axisymmetric RANS and hybrid RANS/PDF calculations to predict the turbulent flow and mixing fields of swirling inert flows and flames. The cases studied, N29S054 and SM1 respectively, are bluff body burner flows, studied experimentally at Sydney University. Turbulence is modeled with a non-linear k-ε type model, taking into account effects of rotation and streamline curvature on the turbulence. Flow field predictions are in reasonable agreement with experimental data. For the reacting flow, agreement for mean mixture fraction and mixture fraction variance with experimental results is less satisfactory. Yet, the mean temperature field is quite well reproduced. We compare presumed and transported scalar PDF simulation results, with the same laminar flamelet model for chemistry. The influence of the micro-mixing model is small in our case. The mixing model constant C_ϕ, has a stronger influence, through the mixture fraction variance.

Introduction

Swirl-stabilized turbulent flames are relevant for a lot of industrial applications, e.g. gas turbines, furnaces, because of their specific advantages compared to non-swirling turbulent flames. The swirling flow in these flames creates recirculation zones which enhance mixing and stabilize the flame. This leads to better combustion efficiency and less pollutant formation. However, swirl flames are quite complex and not yet totally understood. One of the complex phenomena involved in swirl flames is vortex breakdown which leads to flow instability, i.e. precessing vortex core and periodically expanding/shrinking recirculation zone.

Several numerical techniques have been used to simulate these complex flows. The unsteady 3D effects are normally better handled by LES than RANS, but on the other hand LES calculations have a higher computational cost. Therefore, we consider it still useful to study the limitations of RANS and hybrid RANS/PDF calculations in these highly challenging swirling flows, in particular for cases where there is no strong influence from a precessing vortex core (PVC).

A study has already been performed in e.g. [1], but not yet for the Sydney Swirl burner, which was derived from the well-known Sydney bluff-body burner[2]. Experiments have been performed at Sydney University and Sandia National Laboratories [3-7]. The Sydney swirl burner has also been studied numerically by several authors. Masri *et al.* [8] performed a joint velocity-scalar-frequency PDF calculation for a reacting case with the Sydney Bluff Body Burner. LES simulations of non-reacting and reacting cases have been reported by Malalasekera *et al.* [9,10], Stein and Kempf [10,11] and El-Asrag and Menon [12].

Our research started with a preliminary study of the cases in the commercial code FLUENT. This preliminary study consisted of steady 2D axisymmetric and unsteady 3D RANS simulations with the 'realizable *k*-ε model' [13] and with the LRR-IP Reynolds Stress model [14]. In the 3D RANS simulations with LRR-IP, a precessing vortex core was observed. Yet, both in 3D and 2D, the realizable *k*-ε model lead to better agreement with experimental data for the turbulent flow fields than the LRR-IP model. However, care must be taken not to generalize these findings.

Motivated by the results of our preliminary study, we perform in the present paper RANS calculations with the non-linear *k*-ε model of [15], which behaves, at least far away from walls, similarly to the realizable k-ε model. The advantage of this 2D axisymmetric approach is that we can also perform transported scalar PDF (probability density function) simulations, in order to study turbulence – chemistry interaction. At present, we restrict ourselves to a single laminar flamelet model, though. More advanced, finite rate chemistry reduced models like REDIM [16] will be used in future work.

First of all, the performance of the non-linear *k*-ε model is tested in a non-swirling case N29S054. Next, the effect of the turbulent Schmidt number in the mixture fraction (mean and variance) transport equation is reported for the presumed PDF calculations. Finally, we discuss the influence of the micro-mixing model and the model constant C_φ on the transported scalar PDF results.

Experimental Set-up

Figure 1 depicts the burner. The bluff body (50mm diameter) contains the central fuel jet (3.6mm diameter). Swirling air is provided through a 5mm wide annulus

1* Corresponding author: reni.demeester@ugent.be

surrounding the bluff-body. The swirl component is created by air entering through 3 tangential ports. The burner is placed inside a wind tunnel with a square cross section. The velocity measurements were done at Sydney University in a wind tunnel with 130mmx130mm cross section, while the composition measurements were done at Sandia National Laboratories, in a wind tunnel with 310mmx310mm cross section.

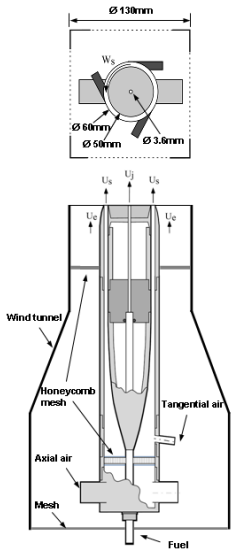

Figure 1: Sydney Swirl Burner (adapted from [17]).

A wide range of testing conditions has been examined experimentally [3-7]. All cases are characterized by: the bulk axial velocity of the central jet (U_j), the bulk axial and tangential velocity of the swirling air annulus (U_s and W_s) and the bulk axial velocity of the co-flow of the wind tunnel (U_e). We consider two specific cases: the inert swirling flow N29S054, in which the central jet consists of air; and the swirling flame SM1, where the central jet consists of CNG. Their flow parameters are summarized in table 1. Also reported in this table is the swirl number which is here geometrically defined as $S_g=W_s/U_s$.

Case	Fuel	U_e (m/s)	U_j (m/s)	U_s (m/s)	W_s (m/s)	S_g
N29S054	Air	20	66	29,7	16	0,54
SM1	CNG	20	32,7	38,2	19,1	0,5

Table 1: Flow parameters of N29S054 and SM1.

The flow field of N29S054 contains 2 recirculation zones: one close to the bluff body and one further downstream near the central axis. The former is caused by the bluff body, while the latter is caused by vortex breakdown. The recirculation zones are separated by a region of high shear stress which coincides with a highly rotating collar. In [7], this highly rotating collar is believed to be responsible for the vortex breakdown, creating the second recirculation zone.

The flow field of SM1 has the same features as N29S054. Local extinction occurs in the region of high shear stress between the two recirculation zones. The hot, re-circulated combustion products from the second recirculation zone cause re-ignition. In the experiments, velocity measurements were performed with CNG, while CH_4 was used for the composition measurements. No physical changes were reported, changing between the fuels.

Numerical Description and Modeling

All calculations are steady 2D axisymmetric and are performed with the same code PDFD, developed at TU Delft [18]. In the past, PDFD has already successfully been applied to non-swirling cases with the Sydney Bluff Body Burner [19].

The 0.3m long computational domain starts at the burner exit. In radial direction, it is 0.15m wide. A non-uniform rectangular grid of 160x128 cells is used.

Boundary conditions for the inlets were generated based on separate calculations inside the burner (performed with Fluent, using the LRR-IP model). The turbulence levels, however, were far too low, compared to the experimental results close to the burner. Therefore, the profiles of turbulent kinetic energy (k) were scaled up to the level of the experimental values. We chose to keep the turbulent frequency ω constant, so that the turbulent dissipation rate ε also had to be scaled up proportional with k. An alternative method to determine ε, is to assume equality of production and dissipation of k and use the definition of the production to determine ε. In first order this also leads to a proportional relationship between k and ε. We do not go into further detail here. The bluff-body was simulated as a slip wall.

The non-linear k-ε turbulence model of [15] is used, as it takes into account the effect of streamline curvature and rotation on turbulence.

The combustion model used for the reacting case is the steady flamelet model. A single flamelet with strain rate of $100s^{-1}$ is calculated in the opposed-flow diffusion flame configuration with OPPDIF [20] using the detailed mechanism GRI2.11. Comparison to results with multiple flamelets, in a presumed β-PDF calculation (in Fluent), revealed no significant differences.

For turbulence – chemistry interaction, we compare two approaches. The first approach is the standard pre-assumed β-PDF method, with the standard transport equation for mean mixture fraction and mixture fraction variance. The second approach concerns the transported scalar PDF approach. The mass density function $F_\Phi(\psi)=\rho(\psi)f_\phi(\psi)$, then obeys the following transport equation [21]:

$$\frac{\partial F_\varphi}{\partial t}+\frac{\partial \widetilde{v}_j F_\varphi}{\partial x_j}+\frac{\partial}{\partial \psi_\alpha}[S_\alpha(\psi)F_\varphi] \qquad (1)$$

$$=\underbrace{-\frac{\partial}{\partial x_j}\left[\left\langle v_j''\middle|\psi\right\rangle F_\varphi\right]}_{\text{gradient diffusion}}-\frac{\partial}{\partial \psi_\alpha}\left[\underbrace{\frac{1}{\rho(\psi)}\left\langle -\frac{\partial J_j^\alpha}{\partial x_j}\middle|\psi\right\rangle}_{\text{mixing model}}F_\varphi\right]$$

In this general equation, S_α is the reaction source term for scalar φ_α and $\boldsymbol{J_\alpha}$ its molecular flux. We only consider one single scalar, namely mixture fraction. As this is a conserved scalar, there is no chemical source term. The two terms at the right hand side need to be modeled. We apply the gradient diffusion model for the turbulent diffusion flux and compare two micro-mixing models: the Modified Curl's coalescence/dispersion model (CD) [22] and the Euclidean Minimum Spanning Tree model (EMST) [23-24]. With CD, all particles can interact with each other in a pair-wise manner, while EMST contains a 'localness principle': particles can only interact with particles that are 'close-by' in mixture fraction space. We use the Lagrangian method to solve eq. (1). Thus, the MDF is represented by a large number of computational particles. The evolution of the particles in mixture fraction space is then calculated by solving the following differential equation for each of the particles:

$$d\xi^* = \underbrace{\theta_\xi(\varepsilon^*,t)}_{\text{micromixing}}dt \qquad (2)$$

The superscript * refers to the fact that the value corresponds to a single numerical particle. Transport in mixture fraction space is thus only caused by micro-mixing.

Results and Discussion

First of all, we discuss results for the inert swirling case (N29S054). Figures 2 and 3 reveal that agreement of the predicted flow field with experimental data is reasonable, partly due to the acceptable prediction of shear stresses <*u'v'*> (Fig. 4) . The 2 recirculation regions are predicted, but their position and size, however, is not completely correct (Fig. 2). Note that, in the 2D axisymmetric steady simulations, the vortex breakdown cannot be accurately captured. Interestingly, although the results for the non-linear model are generally better, even the standard *k-ε* model does quite a good job for this complex case.Over-all, the quality of the turbulent flow field results in the inert case, allows to move on to the reacting cases.

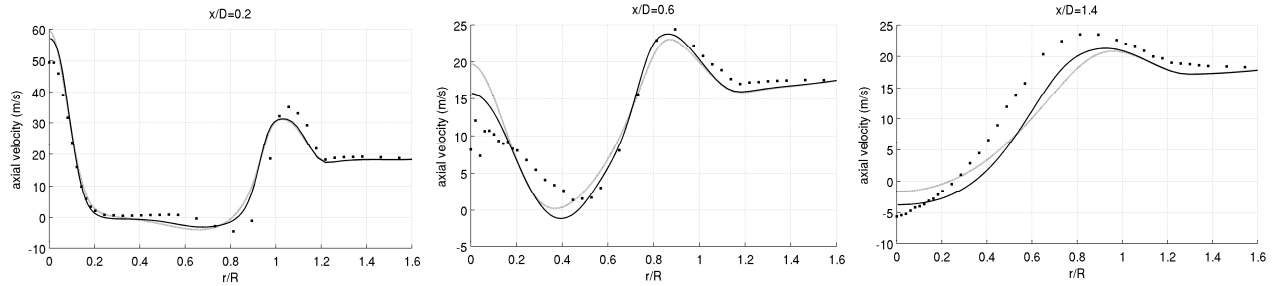

Figure 2: Axial velocity profiles of N29S054: —— non-linear *k-ε*, ····· standard *k-ε*, ▪ exp

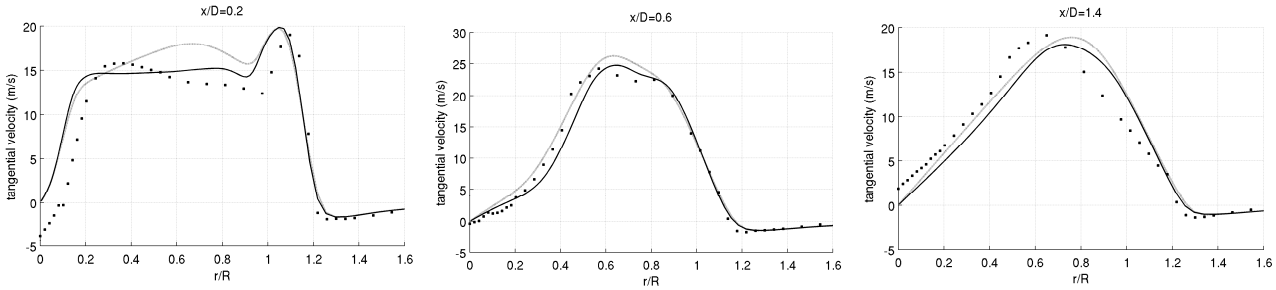

Figure 3: Tangential velocity profiles of N29S054: —— non-linear *k-ε*, ····· standard *k-ε*, ▪ exp

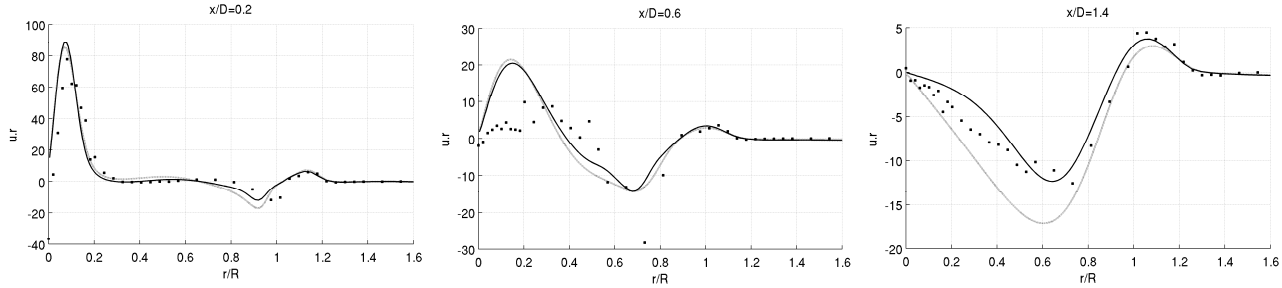

Figure 4: Shear stress <u'v'> profiles of N29S054: —— non-linear *k-ε*, ····· standard *k-ε*, ▪ exp

For SM1, calculations were done first with a presumed *β-PDF* to assess the performance of the non-linear *k-ε* model. We also investigate the influence of the turbulent Schmidt number in the turbulent diffusivity (μ_t/σ_ξ) for scalars. In general, the flow field is well predicted again (Fig. 5 and 6). The influence of the turbulent Schmidt number on the flow field is small. This is expected, as the influence is indirect (through the temperature and density field). With σ_ξ=*0.85*, there is less turbulent diffusion (of mean mixture fraction) and less production of mixture fraction variance for the same level of turbulence. This leads to sharper gradients in the radial profiles for mean mixture fraction (and mixture fraction variance). These sharper gradients result in higher mixture fraction variance values (see e.g. at x = *1.5D*). The mean mixture fraction and mixture fraction variance fields are better predicted for σ_ξ=*0.70*. This directly affects the mean temperature field, which is also better predicted with σ_ξ=*0.70* (not shown). For σ_ξ=*0.85,* the flow fields are very similar (slightly better).

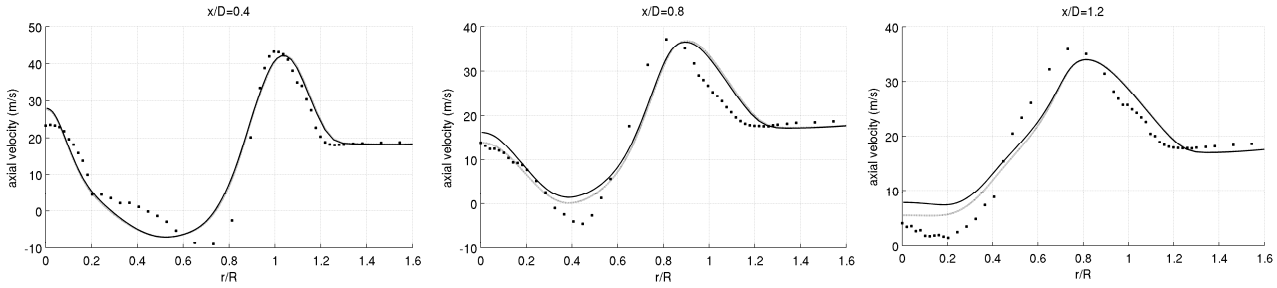

Figure 5: Axial velocity profiles of SM1 for presumed calculations: —— σ_ξ=*0.70,* ····· σ_ξ=*0.85*, ▪ exp

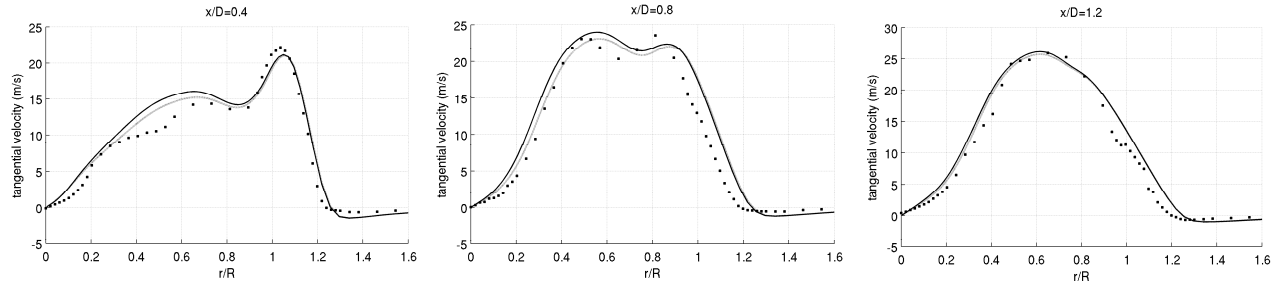

Figure 6: Tangential velocity profiles of SM1 for presumed calculations: —— σ_ξ=*0.70,* ····· σ_ξ=*0.85*, ▪ exp

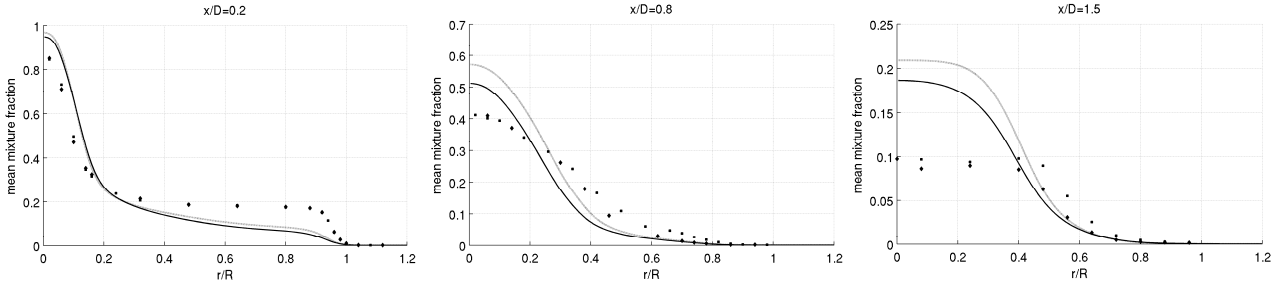

Figure 7: Mean mixture fraction profiles of SM1 for presumed calculations: —— σ_ξ=*0.70,* ····· σ_ξ=*0.85*, ▪ exp

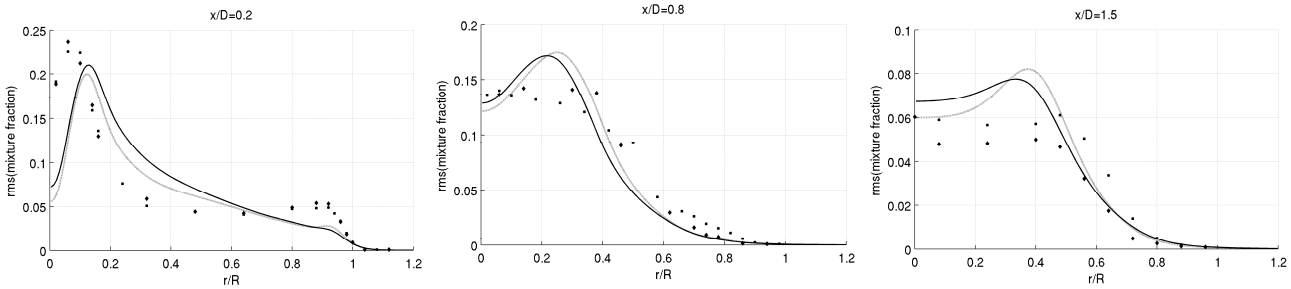

Figure 8: Mixture fraction rms profiles of SM1 for presumed calculations: —— σ_ξ=*0.70,* ····· σ_ξ=*0.85*, ▪ exp

Next, transported joint scalar PDF calculations were performed with σ_ξ=*0.70*. The influence of the micro-mixing model is studied. With the EMST model, the influence of C_ϕ is studied.

The influence of the mixing model on the mean mixture fraction field is clearly very small. This is as expected, as we use a single laminar flamelet for combustion model. Thus, there is no local extinction. Differences in mean density are thus small. This also explains why differences with the pre-assumed PDF results are quite small.

The influence of C_ϕ is clearly visible in Fig. 10, showing the mixture fraction rms. C_ϕ indeed has a direct effect on the mixture fraction rms through the scalar dissipation rate. A lower value of C_ϕ results in a lower mixture fraction variance decay rate and thus to higher mixture fraction variance values, in particular close to the burner. This in turn results in higher temperature fluctuations and lower mean temperatures. However, the main reason for the lower mean temperatures for C_ϕ=*1.5* at *x/D=0.4* and *x/D=0.8* is the lower mean mixture fraction and the highly non-linear behavior of the flamelet model around the stochiometric mixture fraction. Consequently, the central jet slows down more rapidly due to higher shear stresses caused by the higher density (not shown), which then leads to more rapid decay of mean mixture fraction on the axis (Fig. 9). Note that, most probably, when local extinction can occur due to finite rate chemistry, results for the transported PDF might further improve. This is ongoing research.

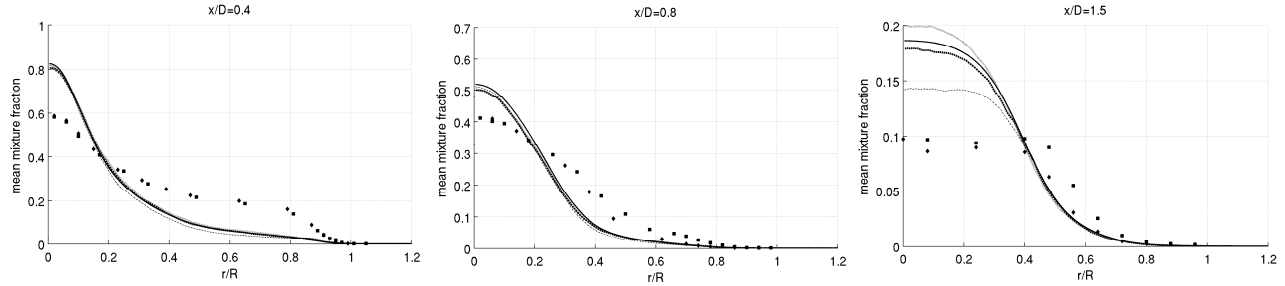

Figure 9: Mean mixture profiles of SM1 for transported scalar PDF calculations:
—— presumed C_ϕ=*2* , —— CD C_ϕ=*2*, ... EMST C_ϕ=*2*, ... EMST C_ϕ=*1.5*, ■ ◆ exp

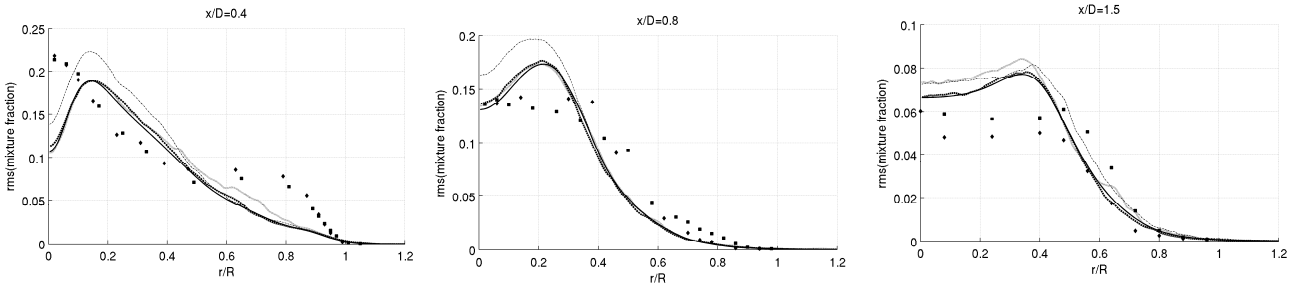

Figure 10: Mixture fraction rms profiles of SM1 for transported scalar PDF calculations:
—— presumed C_ϕ=*2* , —— CD C_ϕ=*2*, ... EMST C_ϕ=*2*, ... EMST C_ϕ=*1.5*,, ■ ◆ exp

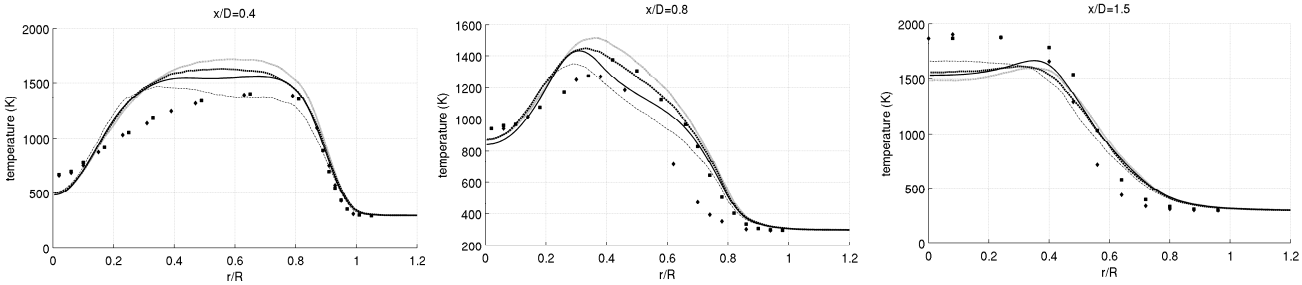

Figure 11: Temperature profiles of SM1 for transported scalar PDF calculations:
—— presumed C_ϕ=*2* , —— CD C_ϕ=*2*, ... EMST C_ϕ=*2*, ... EMST C_ϕ=*1.5*,, ■ ◆ exp

Conclusions

Steady 2D axisymmetric RANS calculations with a non-linear k-ε model were performed for an inert and reacting swirling flow behind a bluff-body burner. For both cases, the turbulent flow predictions are in good agreement with experimental data.

For the reacting case, presumed β-PDF and transported scalar PDF calculations were performed, using the same laminar flamelet model. The influence of the micro-mixing model is small. The mixing constant C_ϕ has a larger influence, through the mixture fraction variance. The best results were obtained with EMST and $C_\phi = 1.5$. It remains to be investigated whether this is still true when finite rate chemistry is considered.

Acknowledgements

This work is funded by the Special Research Fund of Ghent University.

References

[1] Wegner, Maltsev, Schneider, Sadiki, Dreizler, Janicka, Int. Journal of Heat and Fluid Flow 25, (2004) 528-536

[2] B.B.Dally, A.R.Masri, R.S.Barlow and G.J.Fiechtner, Combustion and Flame 114 (1998) 119-148.

[3] Y.M.Al-Abdeli and A.R.Masri, Experimental Thermal and Fluid Science 27 (2003) 655-665.

[4] P.A.M.Kalt, Y.M.Al-Abdeli, A.R.Masri and R.S.Barlow, Proceedings of the Combustion Institute 29 (2002) 1913-1919.

[5] A.R.Masri, P.A.M.Kalt and R.S.Barlow, Combustion and Flame 137 (2004) 1-37.

[6] Y.A.Al-Abdeli, A.R.Masri, G.R.Marquez and S.H.Starner, Combustion and Flame 146 (2006) 200-214.

[7] A.R.Masri, P.A.M.Kalt, Y.M.Al-Abdeli and R.S.Barlow, Combustion Theory and Modelling 11 (2007) 653-673.

[8] A.R.Masri, S.B.Pope and B.B.Dally, Proceedings of the Combustion Institute 28 (2000) 123-131.

[9] W.Malalasekera, K.K.J.Ranga-Dinesh, S.S.Ibrahim and A.R.Masri, Combustion Science and Technology 180 (2008) 809-832.

[10] A.Kempf, W.Malalasekera, K.K.J.Ranga-Dinesh and O.Stein, Flow Turbulence and Combustion 81 (2008) 523-561.

[11] O.Stein and A.Kempf, Proceedings of the Combustion Institute 31 (2007) 1755-1763.

[12] H.El-Asrag and S.Menon, Proceedings of the Combustion Institute 31 (2007) 1747-1754.

[13] T.-H. Shih, W.W. Liou, A. Shabbir, Z. Yang, J. Zhu,
Computers Fluids 24 (3) (1995) 227–238.

[14] B.E. Launder, G.J. Reece, W. Rodi, J. Fluid Mech. 68 (1975) 537–566.

[15] B.Merci and E.Dick, International Journal of Heat and Mass Transfer 46 (2003) 469-480.

[16] V. Bykov, U. Maas, Combustion Theory and Modelling 11(2007) 839–862.

[17]http://www.aeromech.usyd.edu.au/thermofluids/swirl_files/burner-plan.pdf

[18] B.Naud, C. Jimenez, D. Roekaerts, Progress in Computational Fluid Dynamics 6 (1-3) 146-157

[19] B.Merci, D.Roekaerts, B.Naud and S.B.Pope, Combustion and Flame 146 (2006) 109-130

[20] A.E. Lutz, R.J. Kee, J.F. Grcar, F.M. Rupley, Technical Report SAND96-8243, UC-1409, Sandia National Laboratories (1996).

[21] S.B.Pope, Progress in Energy and Combustion Science 11 (1985) 119-192.

[22] J. Janicka, W. Kolbe, W. Kollman, J. Non-Equil. Thermodyn.4 (1979) 47–66.

[23] S. Subramaniam, S.B. Pope, Combust. Flame 115 (1998) 487–514.

[24] S. Subramaniam, S.B. Pope, Combust. Flame 117 (4) (1999) 732–754.